Optical Engineering

SPIEDigitalLibrary.org/oe

Technique for passive scene imaging of gas and vapor plumes using transmission-waveband modulation

David M. Benton

Technique for passive scene imaging of gas and vapor plumes using transmission-waveband modulation

David M. Benton
L-3 TRL Technology, Unit 19 Miller Court, Severn Drive, Tewkesbury, Gloucestershire GL20 8DN, United Kingdom
E-mail: david.benton@l-3com.com

Abstract. A new approach to locating gas and vapor plumes is proposed that is entirely passive. By modulating the transmission waveband of a narrow-band filter, an intensity modulation is established that allows regions of an image to be identified as containing a specific gas with absorption characteristics aligned with the filter. A system built from readily available components was constructed to identify regions of NO_2. Initial results show that this technique was able to distinguish an absorption cell containing NO_2 gas in a test scene. © *2012 Society of Photo-Optical Instrumentation Engineers (SPIE).* [DOI: 10.1117/1.OE.51.5.050501]

Subject terms: spectroscopy; dielectric filters; modulation; image processing.

Paper 111571L received Dec. 15, 2011; revised manuscript received Feb. 27, 2012; accepted for publication Apr. 5, 2012; published online May 4, 2012.

1 Introduction

Passive techniques for spectroscopic identification[1] rely on changes in the background light levels to expose the presence of chemicals. Combined with imaging, this enables a wide field of view to be constantly examined. Although target gas concentration levels may be low, the absorption paths can be very long (several kms) enabling detection with high sensitivity.[2] Video technology has been used for imaging anthropogenic gas distributions[3,4] such as NO_2 and SO_2. Typically this has been achieved using Fourier transform infrared (FTIR) spectroscopy techniques,[5] which are scanning rather than direct-imaging techniques.

Tuning a filter across an absorption induces an intensity modulation for light that has travelled via the absorbing gas. This technique is normally performed by tuning the source, such as in tunable diode laser spectroscopy.[6] This technique can be applied to an entire image and the modulation regions (or pixels) of a scene containing the absorber can be identified. The approach proposed here utilizes a well-established optical technique[7] of tilting a dielectric interference filter to translate the pass band to shorter wavelength. The filter central transmission wavelength λ as a function of tilt angle θ is:

$$\lambda(\theta) = \lambda(0)\left[1 - \left(\frac{1}{n_e}\right)^2 \sin(\theta)^2\right]^{1/2},$$

where n_e is the effective refractive index.

2 Direct Scene Viewing

In order to prove rapidly this technique the choice of analyte gas is essential, having absorption features in the visible region of the spectrum that match well with commercially available narrow-band filters, hence NO_2 was chosen. Absorption cross-section data for NO_2 were obtained from the work done in Ref. 8. Filters centered at 490 nm [10 nm full width at half maximum (FWHM)] and 488 nm (3 nm FWHM) were acquired. The total absorption cross-section viewed through each filter was calculated for angle tilts up to 30°. The wider bandwidth filter integrates across more of the spectrum and averages out intrinsic variations in the absorption spectrum hence results in smaller relative modulations of the transmitted intensity. The expected attenuation with tilt angle for filters around 490 nm is shown in Fig. 1. The experimental arrangement is shown schematically in Fig. 2. The filter is mounted on a universal serial bus (USB)-controlled servo (Robotis RX-10) and the camera is a complementary metal-oxide semiconductor (CMOS) monochrome USB camera (ThorLabs, DCC1240M). Both the servo and camera are controlled via a LabView program.

A cylindrical absorption cell (8 mm diameter, with NO_2 at 400 mBar) can be seen as a central horizontal strip in the camera image seen in the inset image of Fig. 3. The scene is back lit, and to balance the intensity profile (i.e., to mitigate against intensity dependent effects), neutral absorbers are placed on either side of the cell, with different levels of absorption above and below the cell. The filter was oscillated through 0 to 20° with a saw-tooth function at a rate of 1 Hz and frames were collected at a rate of 10 frames per second. Frame buffers of up to 60 frames were then processed as follows. To improve processing speed the images were scaled down in size. A reference signal was obtained by averaging the intensity in a central region of the image that is known not to contain NO_2. This was done because the transmission through the filter drops as the filter angle is increased and also the detection efficiency of the camera is reduced as the wavelength gets shorter. Hence the whole image modulates with filter angle and it is necessary to establish which parts of the image are modulating differently with respect to the reference signal. The image of a white light-emitting diode (LED) was introduced with a pellicle beamsplitter and used to correct the images for tilt-induced lateral offsets. The intensity time series for each pixel was then normalized and compared with a normalized reference signal. From this a single image was produced representing the modulation behavior, with intensity values representing suitably scaled comparison values.

3 Results

Several methods were attempted for comparison of the modulating reference time series $R(t)$ and signal $S(t)$ for each pixel. The most promising for exposing target gas regions were calculations of the covariance coefficient $\mathrm{Cov}[R(t), S(t)]$, the Pearson correlation coefficient $\mathrm{Cov}[R(t), S(t)]/\sigma_R\sigma_S$ and a variation that calculates $\mathrm{Cov}[R(t) - S(t)], [1 - R(t)]$. Results for different image-processing techniques with two filters of different bandwidths are shown in Fig. 3. The intensity of each pixel in the processed image represents the calculated scalar value of the covariance (or correlation) coefficient formed between $R(t)$ and $S(t)$ across a set of video frames at each pixel location. The different temporal behavior

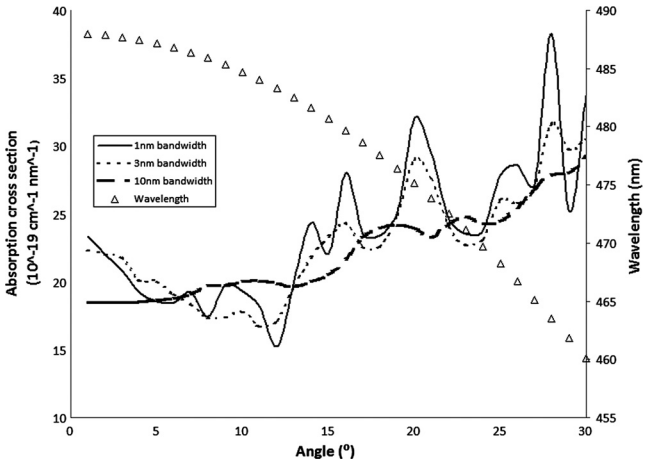

Fig. 1 Expected variation in integrated absorption cross-section versus filter tilt angle, normalized for filter transmission bandwidth for a 488-nm filter with bandwidths of 1, 3 and 10 nm. The filter central transmission wavelength is also shown with the scale on the right.

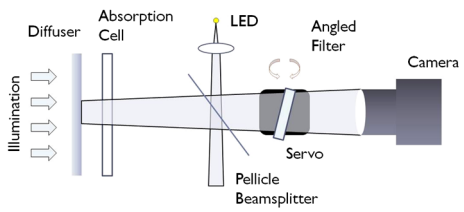

Fig. 2 Schematic diagram of the experimental arrangement.

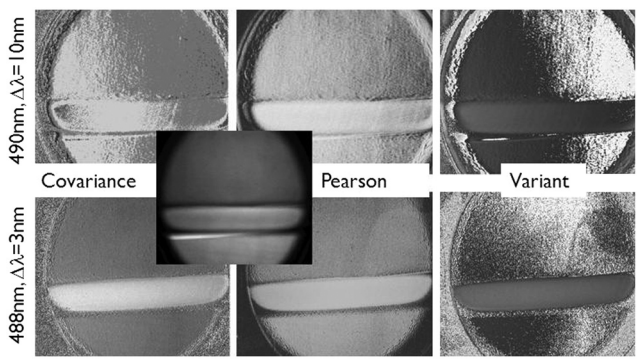

Fig. 3 Processed results from a series of 60 frames during filter modulation using different filters and various processing methods. Inset is the unprocessed scene at a fixed angle.

of the pixel intensities in the absorption-cell region results in visible discrimination of the absorption cell. Such discrimination is clearly dependent upon suitable scaling of the image to reveal sufficient contrast differences.

This technique was also applied to a more general scene containing the absorption cell with a less controlled approach to illumination levels and the results are shown in Fig. 4. The absorption cell shows up as the bright vertical stripe on the right hand side of the processed image. Best results were

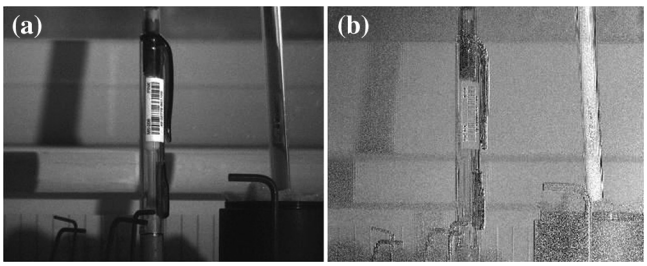

Fig. 4 Scene containing an absorption cell (a) and a processed result (b) revealing the NO_2 absorption cell as the bright vertical structure on the right-hand side.

obtained with a tilt range of 10 to 20° with the 3 nm bandwidth filter, corresponding to the largest change in attenuation, as seen in Fig. 1.

4 Conclusion

The system as presented has the merit of being extremely simple to implement by placing the titling filter system in front of any camera (suitably sensitive) and subsequently processing the video in real time or offline. It is therefore a very cost-effective implementation as both the filter and the servo are low cost and could offer a route to imaging the spatial and temporal evolution of pollutants. This approach could clearly benefit significantly from image-processing techniques that improve the sensitivity beyond detecting what are relatively large absorbers, and indeed this is necessary if this is to find wider application. Tilting filters are far from ideal as they lead to image shifts which have been corrected in software. They also lead to angular differences in the transmission angle through the filter across the image, which will make interpreting the image results more complicated. Nevertheless it can be seen that this simplistic implementation works. Development of this system will concentrate on improving the sensitivity through improved processing and optimizing the optical system.

References

1. W. Markus Sigrist, *Air Monitoring by Spectroscopic Techniques*, Vol. **127**, Wiley, New York (1994).
2. R. T. Ku, E. D. Hinkley, and J. O. Sample, "Long-path monitoring of atmospheric carbon monoxide with a tunable diode laser system," *Appl. Opt.* **14**(4), 854–861 (1975).
3. V. S. Davydov and A. V. Afonin, "Developing video spectroradiometer-gas-viewers for determining the spatial distribution of anthropogenic gases in the near-earth atmosphere and the results of a full-scale experiment," *J. Opt. Technol.* **74**(2), 100–106 (2007).
4. A. V. Afonin, N. M. Drichko, and I. N. Sivyakov, "Wide-angle interference-polarization filter of a video spectroradiometer-gas viewer for recording nitrogen dioxide," *J. Opt. Technol.* **71**, 776–779 (2004).
5. A. Beil et al., "Remote sensing of atmospheric pollution by passive FTIR spectrometry," *Proc. SPIE* **3493**, 32–43 (1998).
6. W. Demtröder, *Laser Spectroscopy: Basic Concepts and Instrumentation*, pp. 296–302, Springer, Berlin (2003).
7. S. A. Pollack, "Angular dependence of transmission characteristics of interference filters and application to a tenable fluorometer," *Appl. Opt.* **5**(11), 1749–1756 (1966).
8. A. C. Vandaele et al., "Fourier transform measurement of NO2 absorption cross-section in the visible range at room temperature," *J. Atmos. Chem.* **25**(3), 289–305 (1996).